Dyes and Pigments 89 (2011) 29–36

Contents lists available at ScienceDirect

Dyes and Pigments

journal homepage: www.elsevier.com/locate/dyepig

Orange phosphorescent organic light-emitting diodes based on spirobenzofluorene type carbazole derivatives as a host material

Young-Min Jeon [b], In-Ho Lee [a], Hyun-Seok Lee [a], Myoung-Seon Gong [a,b,*]

[a] Department of Nanobiomedical Science and WCU Research Center of Nanobiomedical Science, Dankook University, Chungnam 330-714, Republic of Korea
[b] Department of Chemistry and Institute of Basic Science, Dankook University, Chungnam 330-714, Republic of Korea

ARTICLE INFO

Article history:
Received 27 June 2010
Received in revised form
22 August 2010
Accepted 25 August 2010
Available online 28 September 2010

Keywords:
Carbazole
PHOLED
Phosphorescent
Spiro[fluorene-benzofluorene]
Orange host

ABSTRACT

Spiro-type orange phosphorescent host materials, 9-carbazole-spiro[benzo[c]fluorene-7,9′-fluorene] (**OPH-1C**) and 5-carbazole-spiro[benzo[c]fluorene-7,9′-fluorene] (**OPH-2C**) were designed and successfully prepared by the amination reaction. The EL characteristics of **OPH-1C** and **OPH-2C** as orange host materials doped with iridium(III) bis(2-phenylquinoline)acetylacetonate ($Ir(pq)_2acac$) were evaluated. The electroluminescence spectra of the indium tin oxide (ITO, 150 nm)/*N,N′*-diphenyl-*N,N′*-bis-[4-(phenyl-m-tolyl-amino)-phenyl]-biphenyl-4,4′-diamine (DNTPD, 60 nm)/*N,N′*-di(1-naphthyl)-*N,N′*-diphenylbenzidine (NPB, 30 nm)/9-carbazole-spiro[benzo[c]fluorene-7,9′-fluorene] (**OPH-1C**): $Ir(pq)_2acac$ (30 nm, 3%)/2,9-dimethyl-4,7-diphenyl-1,10-phenanthroline(BCP, 5 nm)/tris(8-hydroxyquinoline)aluminum (Alq_3, 20 nm)/LiF (1 nm)/Al (200 nm) devices show a narrow emission band with a full width at half maximum of 73 nm and a $\lambda_{max} = 596$ nm. The device obtained from **OPH-1C** doped with 3% $Ir(pq)_2acac$ showed an orange color purity of (0.595, 0.387) and efficiency of 17.6 cd/A at 6.0 V.

1. Introduction

Organic light-emitting diodes (OLEDs) have been the focus of both academic research and industrial interest in the past two decades, because of their potential application in flat-panel displays and solid lighting resources [1–5]. In particular, intensive studies have been conducted on the development of transitional metal complex based phosphorescent OLEDs (PHOLEDs), owing to their potential ability to achieve an internal quantum efficiency of 100% by harvesting both singlet and triplet excitons [6]. However, orange PHOLEDs are challenging, because of the difficulty of finding a suitable host material with an E_T (triple energy) exceeding that of the commonly used orange phosphorescent dyes. Orange phosphorescent dyes can be used for white organic light-emitting diodes (WOLEDs). White OLED (WOLED) technology can replace the back lights used in LCDs owing to their potential as low-cost and large-area full color displays and solid-state lightings. From the standpoint of their environment friendliness and low electric consumption, WOLEDs constitute a good candidate for high efficiency light units [7–9]. However, it was not until the discovery of organic phosphorescent materials that researchers began seriously looking into the possibility of using WOLEDs for thin-film solid state lighting. Recent results have shown continually improved WOLEDs, which are now surpassing incandescent lamps in terms of their efficiency and lifetime [10]. Carbazole derivatives are photoconductors with good hole-transport properties [11–14]. Recently, carbazole based host materials have been effective as host materials for deep blue PHOLEDs due to the high triplet energy of the carbazole unit [15,16]. However, more studies are required to develop high efficiency deep blue PHOLEDs.

The spirobifluorene and spirosilabifluorene derivatives were widely used for new amorphous host and dopant materials possessing high morphological stability [17–23]. Spirobifluorene with a high glass transition temperature also showed an excellent nondispersive hole transporting and ambipolar carrier transporting properties [24,25]. Recently spirofluorenebenzofluorene would be a useful strategy to expand the application of spiro compounds [26–32].

In this study, new spirobenzofluorene based carbazole compounds were developed and evaluated as red phosphorescent host materials. The devices based on these spiro complexes emit orange light at 593 nm with exceedingly high brightness and external quantum, current and power efficiencies. The device performances of the orange PHOLEDs with the **OPH-1C** and **OPH-2C** hosts were investigated according to the doping concentration of red dopant.

* Corresponding author at: Department of Chemistry and Institute of Basic Science, Dankook University, Chungnam 330-714, Republic of Korea. Tel./fax: +82 41 5501476.
E-mail address: msgong@dankook.ac.kr (M.-S. Gong).

0143-7208/$ – see front matter © 2010 Elsevier Ltd. All rights reserved.
doi:10.1016/j.dyepig.2010.08.015

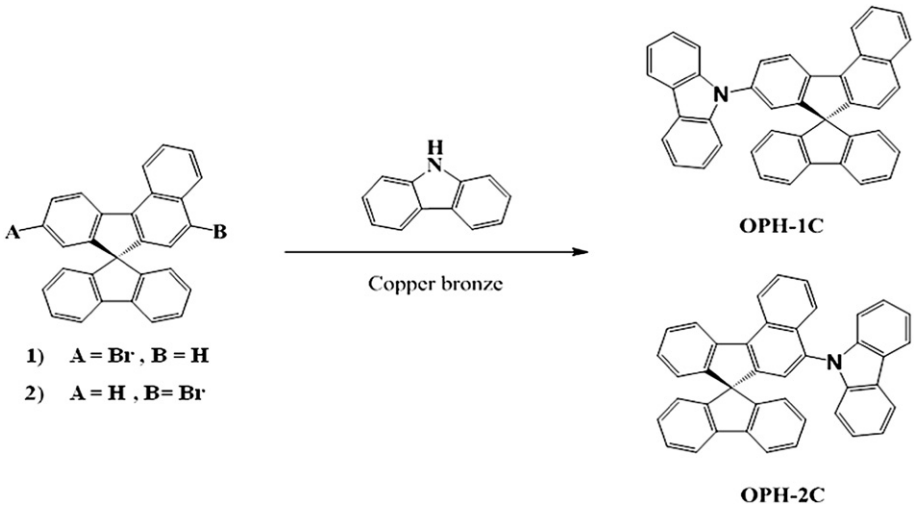

Scheme 1. Chemical structures of Orange phosphorescent host materials.

2. Experimental

2.1. Materials and measurements

Carbazole (95%), potassium carbonate (99%), copper powder (99%), dichloromethane (95%) and nitrobenzene (Aldrich Chem. Co.) were used without further purification. Ammonia water (Duksan Chem. Co.) was used as received. Tetrahydrofuran was distilled over sodium and calcium hydride. 9-bromospiro[benzo[c]fluorene-7,9′-fluorene] and 5-bromospiro[fluorene-7,9′-benzofluorene] were prepared as previously reported [28–30].

The photoluminescence (PL) spectra were recorded on a fluorescence spectrophotometer (Jasco FP-6500) and the UV–vis spectra were obtained by means of a UV–vis spectrophotometer (Shimadzu, UV-1601PC). The energy levels were measured with a low-energy photo-electron spectrometer (Riken-Keiki AC-2). The FT-IR spectra were obtained with a Thermo Fisher Nicolet 850 spectrophotometer and the elemental analyses were performed using a CE Instrument EA1110. The DSC measurements were performed on a Shimadzu DSC-60 differential scanning calorimeter under nitrogen at a heating rate of 10 °C/min. The TGA measurements were performed on a Shimadzu TGA-50 thermo gravimetric analyzer at a heating rate of 5 °C/min. The low and high resolution mass spectra were recorded using a JEOL JMS-AX505WA spectrometer in FAB mode.

2.2. Synthesis of 9-carbazole-spiro[benzo[c]fluorene-7,9′-fluorene] (***OPH-1C***)

A mixture of 9-bromospiro[benzo[c]fluorene-7,9′-fluorene] (5.00 g, 11.23 mmol), carbazole (2.06 g, 12.35 mmol), potassium carbonate (3.1 g, 22.45 mmol) and copper bronze (0.71 g, 11.23 mmol) in nitrobenzene (80 ml) was refluxed with vigorous stirring under a nitrogen atmosphere for 18 h. After the removal of the solvent in vacuo, ammonia solution (80 ml) was added and the mixture was left to stand for 2 h. Dichloromethane (150 ml) and distilled water (100 ml) were then added and the organic layer was separated. After the organic layer was evaporated with a rotary evaporator, the resulting powdery product was purified by column chromatography using a mixture of dichloromethane/hexane (v/v, 1/1) as eluent to give a white crystalline **OPH-1C**.

Yield 64%. Mp 261 °C. ^{1}H-NMR (500 MHz, $CDCl_3$) δ 8.88–8.87 (d, 1H, Ar-CH- benzene), 8.62–8.61 (d, 1H, Ar-CH-carbazole), 8.05–8.04 (d, 2H, Ar-CH-naphthalene), 7.94–7.92 (d, 1H, Ar-CH-carbazole), 7.82–7.81 (d, 2H, Ar-CH-carbazole), 7.75–7.74 (t, 1H, Ar-CH-carbazole), 7.67–7.66 (d, 2H, Ar-CH-benzene), 7.60–7.58 (t, 1H, Ar-CH-fluorene), 7.37–7.34 (t, 2H, Ar-CH-fluorene), 7.34–7.33 (t, 1H, Ar-CH-fluorene), 7.33–7.32 (d, 1H, Ar-CH-carbazole), 7.28–7.22 (m, 1H, Ar-CH-c), 7.20–7.18 (m, 3H, Ar-CH-benzene), 7.18–7.14 (t, 2H, Ar-CH-benzene), 7.11–6.99 (s, 1H, Ar-CH-benzene), 6.87–6.84 (d, 2H, Ar-CH-benzene), 6.84–6.82 (d, 1H, Ar-CH-carbazole), ^{13}C NMR ($CDCl_3$) δ 152.0, 148.2, 147.5, 142.3, 142.1, 140.8, 136.4, 135.9, 134.3, 129.6, 129.4, 128.2, 128.1, 127.3, 126.4, 126.0, 125.9, 124.1,124.0, 123.8, 123.5, 122.7, 122.2, 120.4, 120.4, 120.0, 109.9, 77.4, 77.2, 76.9, 66.4. FT-IR (KBr, cm^{-1}) 3052, 3037 (aromatic C–H), 1268 (aromatic C–N). Anal. Calcd for $C_4H_{25}H$ (Mw, 531.64): C, 92.63; H, 4.74; N, 2.63. Found: C, 92.59; H, 4.68; N, 2.71. MS (FAB) *m/z* 531.6 [$(M+1)^+$]. UV–vis (THF): λ_{max} (Absorption) = 345 nm, λ_{max} (Emission) = 395 nm.

2.3. Synthesis of 5-carbazole-spiro[benzo[c]fluorene-7,9′-fluorene] (***OPH-2C***)

A mixture of 5-bromospiro[benzo[c]fluorene-7,9′-fluorene] (4.00 g, 8.98 mmol), carbazole (1.65 g, 9.88 mmol), potassium carbonate (2.5 g, 17.96 mmol) and copper bronze (0.57 g, 8.98 mmol) in nitrobenzene (70 ml) was stirred and refluxed under a nitrogen atmosphere for 18 h. After the removal of the solvent in vacuo, ammonia solution (70 ml) was added and the mixture was left to stand for 2 h. Dichloromethane (150 ml) and water (100 ml) were added and the organic phase was separated. The organic solution was washed with water (100 ml × 2) twice. After the resulting solution was evaporated with rotary evaporator, the resulting powdery product was purified by column chromatography using a mixture of dichloromethane/hexane (v/v, 1/1) as eluent to give **OPH-2C** as a white solid.

Yield 68%. Mp 371 °C ^{1}H-NMR (500 MHz, $CDCl_3$) δ 9.02–9.00 (d, 1H, Ar-CH- benzene), 8.54–8.52 (d, 1H, Ar-CH-carbazole), 8.11–8.10 (d, 1H, Ar-CH-naphthalene), 8.10–8.09 (d, 1H, Ar-CH-carbazole), 7.78–7.77 (d, 1H, Ar-CH-benzene), 7.76–7.75 (d, 2H, Ar-CH-carbazole), 7.52–7.51 (t, 1H, Ar-CH-benzene), 7.37–7.36 (t, 1H, Ar-CH-carbazole), 7.35–7.34 (d, 3H, Ar-CH-benzene), 7.24–7.23 (t, 1H, Ar-CH-carbazole), 7.23–7.22 (t, 1H, Ar-CH-carbazole), 7.20–7.19 (m, 3H, Ar-CH-fluorene), 7.13–7.12 (d, 2H, Ar-CH-benzene), 7.12–7.11 (s, 1H, Ar-CH-fluorene), 6.96–6.87 (d, 1H, Ar-CH- benzene), 6.83–6.81 (m, 3H, Ar-CH-benzene), 6.84–6.82 (d, 1H, Ar-CH-carbazole), ^{13}C NMR ($CDCl_3$) δ 150.2, 148.1, 147.5, 142.4, 142.3, 142.1, 137.4, 134.2, 131.3, 130.8, 128.2, 128.1, 127.7, 126.6, 126.0, 125.1, 124.6, 124.4, 124.0,

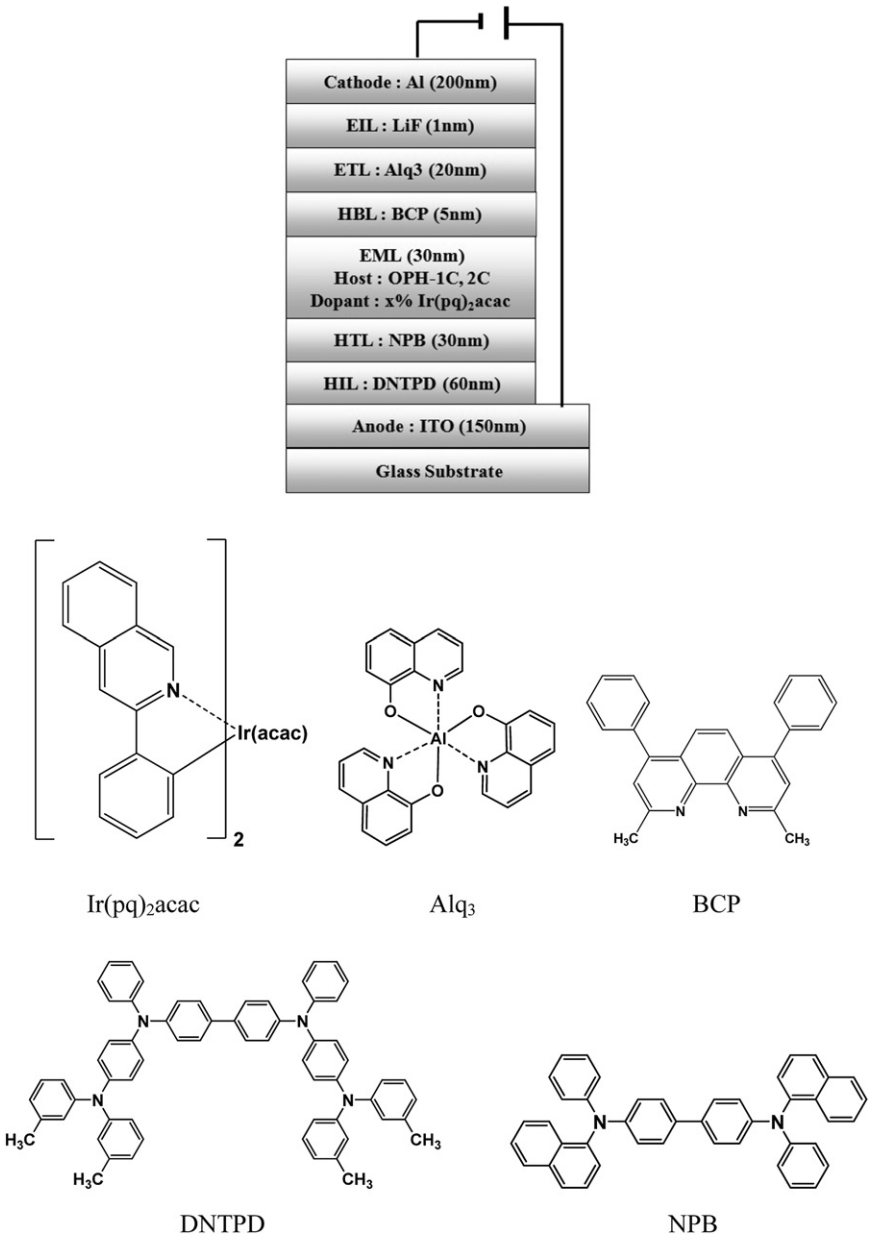

Fig. 1. The device configuration and the chemical structure of the materials used in the devices.

123.4, 123.3, 123.2, 120.4, 120.4, 119.9, 110.3, 77.4, 77.2, 76.9, 66.6. FT-IR (KBr, cm^{-1}) 3054, 3039 (aromatic C–H), 1268 (aromatic C–N). Anal. Calcd for $C_4H_{25}H$ (Mw, 531.64): C, 92.63; H, 4.74; N, 2.63. Found: C, 92.62; H, 4.70; N, 2.70. MS (FAB) *m*/*z* 531.6 $[(M+1)^+]$. UV–vis (THF): λ_{max} (Absorption) = 337 nm, λ_{max} (Emission) = 411 nm.

2.4. PHOLED fabrication

A basic device configuration of indium tin oxide (ITO, 150 nm)/*N*,*N*′-diphenyl-*N*,*N*′-bis-[4-(phenyl-m-tolyl-amino)-phenyl]-biphenyl-4,4′-diamine (DNTPD, 60 nm)/*N*,*N*′-di(1-naphthyl)-*N*,*N*′-diphenylbenzidine (NPB, 30 nm)/**OPH-1C** or **OPH-2C**: $Ir(pq)_2acac$ (30 nm, x %)/2,9-dimethyl-4,7-diphenyl-1,10-phenanthroline (BCP, 5 nm)/tris(8-hydroxyquinoline)aluminum (Alq_3, 20 nm)/LiF (1 nm)/Al (200 nm) was used for the fabrication of the devices. All organic materials except for the dopants were deposited at a deposition rate of 1 Å/s. 1, 3 and 10% doping concentrations of $Ir(pq)_2acac$ were used. The devices were encapsulated with a glass lid and a CaO getter after cathode deposition. The current density–voltage-luminance and electroluminescence characteristics of the blue fluorescent OLEDs were measured with a Keithley 2400 source measurement unit and CS 1000 spectroradiometer, respectively. The measurement of the lifetime of the blue OLEDs was carried out at a luminance of 5000 cdm^{-2} in constant current mode.

3. Results and discussion

3.1. Synthesis and characterization

The key intermediate step in this synthesis is the introduction of carbazole substituent into the 5- or 9-position of the spiro[fluorene-7,9′-benzofluorene] by amination reactions in order to synthesize host materials having good hole-transport properties. The orange

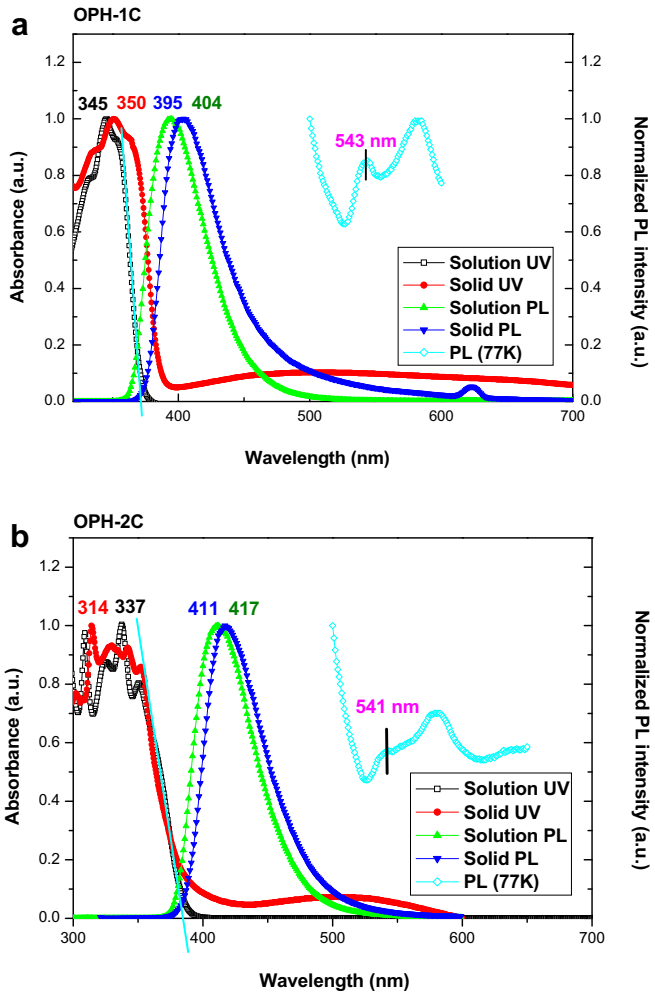

Fig. 2. Normalized absorption and photoluminescence spectra of (a) **OPH-1C** and (b) **OPH-2C** and energy diagram of host material.

host materials, 9-carbazole-spiro[benzo[c]fluorene-7,9′-fluorene] (**OPH-1C**) and 5-carbazole-spiro[benzo[c]fluorene-7,9′-fluorene] (**OPH-2C**), were prepared by the amination reactions of the compounds, 9-bromospiro[fluorene-7,9′-benzofluorene] and 5-bromospiro[fluorene-7,9′-benzofluorene], with carbazole, respectively, in the presence of a copper catalyst. The synthetic routes to the two host materials are described in Scheme 1. The chemical structures and compositions of the resulting precursor and spiro-compounds were characterized by ^{1}H-NMR, ^{13}C-NMR, FT-IR and GC-MS. The chiral carbon peak was observed at 65.5 ppm in the ^{13}C NMR spectra. The results of the elemental analysis and mass spectroscopy also supported the formation of **OPH-1C** and **OPH-2C** and matched well with the calculated data.

3.2. Optical properties and energy levels

The introduction of carbazole to the 5- or 9-positions in spiro [fluorene-benzofluorene] caused a significant red-shift in the PL spectra of **OPH-1C** and **OPH-2C** to 395 and 411 nm, respectively, due to the increased electron donation. UV-vis and PL spectra of the **OPH-1C** and **OPH-2C** are shown in Fig. 2. Although the same spirobifluorene core and carbazole side group were used in the molecular structure, UV-vis absorption spectra of the **OPH-1C** and **OPH-2C** were different in peak shape for both solution and film states. The difference of the absorption pattern in the two host materials is due to the steric hindrance of the spirobenzofluorene group in the **OPH-2C**. As seen in the molecular structure of the **OPH-2C** in Fig. 3, the carbazole structure can be distorted by the spirobezofluorene substituted at 5-position, leading to the reduction of the degree of conjugation of the carbazole [33]. The solution and solid PL spectra of **OPH-2C** were red shifted to 411 and 417 nm compared with those of the **OPH-2C** (395 and 404 nm).

Fig. 4 shows the schematic energy-level alignment of the device. The energy levels of the new host materials were measured by cyclic voltammetry and estimated from their absorption and PL spectra. The triplet energy band gap was measured at 77 K because the triplet state showed a big loss in the presence of oxygen. Triplet energy band gaps of 2.28 and 2.29 eV were observed for **OPH-1C** and **OPH-2C**, respectively. It can be seen that the highest occupied molecular orbital (HOMO) and lowest unoccupied molecular orbital (LUMO) were 6.00 eV and 2.67 eV for **OPH-1C,** and 6.53 eV and 3.31 eV for **OPH-2C**, respectively. The energy barrier for hole injection from the hole transport layer to the orange light emitting layer between NPB and the **OPH-2C** host material in the device obtained from **OPH-2C** was 1.13 eV.

An investigation of the energy diagram is one of the performance evaluations of the orange host materials. The energy diagram of **OPH-2C** (Fig. 4(a)) was quite different from that of **OPH-1C** (Fig. 4(b)). The band gap of dopant Ir(pq)$_2$acac were located in the band gap of the host **OPH-1C**, whereas the LUMO of the host was lower than that of the dopant material. This would not facilitate the energy transfer between the dopant and host, therefore the efficiency of the device was expected to be low.

Molecular simulation of **OPH-1C** and **OPH-2C** was performed to study the molecular orbital distribution of **OPH-1C** and **OPH-2C**. Fig. 5 shows the highest occupied molecular orbital (HOMO) and the lowest unoccupied molecular orbital (LUMO) distribution of **OPH-1C** and **OPH-2C**. The HOMO orbitals of **OPH-2C** were mostly localized in the carbazole unit with little orbital distribution in the

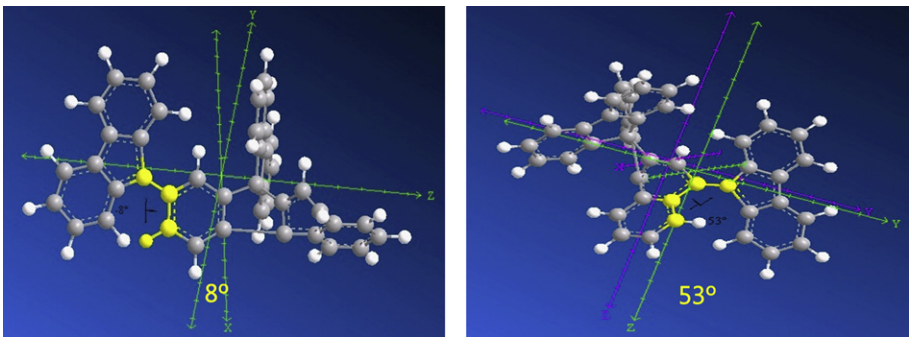

Fig. 3. Optimized geometrical structure of **OPH-1C** and **OPH-2C**.

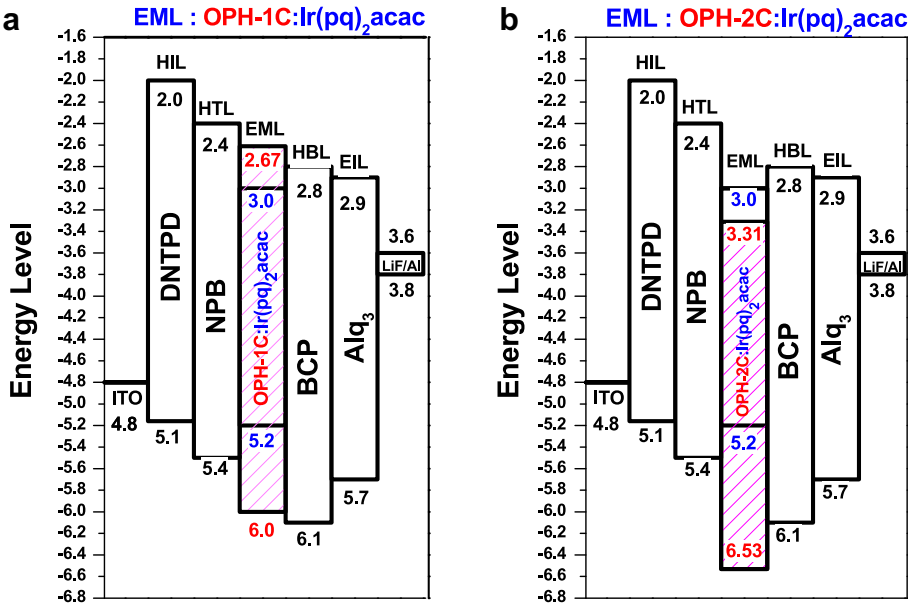

Fig. 4. Energy level diagrams of the (a) **OPH-1C**: Ir(pq)$_2$acac and (b) **OPH-2C**: Ir(pq)$_2$acac devices.

spirobezofluorene. The carbazole group lightly affects the HOMO orbital distribution of the **OPH-2C** compared with that of **OPH-1C**. This indicates that the introduction of the carbazole group to 5-position of spirobenzefluorene was not efficient for the PHOLED. The LUMO distribution of OPH-2C was quite similar to that of **OPH-1C**. The carbazole group was little affected (distorted by 8°, Fig. 3) by the 9-positioned phenyl group of spirobenzofluorene in **OPH-1C**, but it was affected by the 5-positioned naphthalene group of spirobezofluorene in the **OPH-2C**. The carbazole moiety in the **OPH-1C** can be freely rotated, but the rotation of the carbazole group in the **OPH-2C** is limited by the steric hindrance of the spirobenzofluorene. This leads to the distortion of the carbazole core structure (distorted 53°, Fig. 3) and the delocalization with the carbazole group can be destroyed by the spirobenzofluorene group in the **OPH-2C**.

3.3. Thermal properties

The thermal properties of the resulting orange emitting materials were characterized by DSC and TGA in a nitrogen atmosphere. The onset decomposition temperatures were 466 and 458 °C for **OPH-1C** and **OPH-2C**, respectively. Table 1 summarizes the DSC and

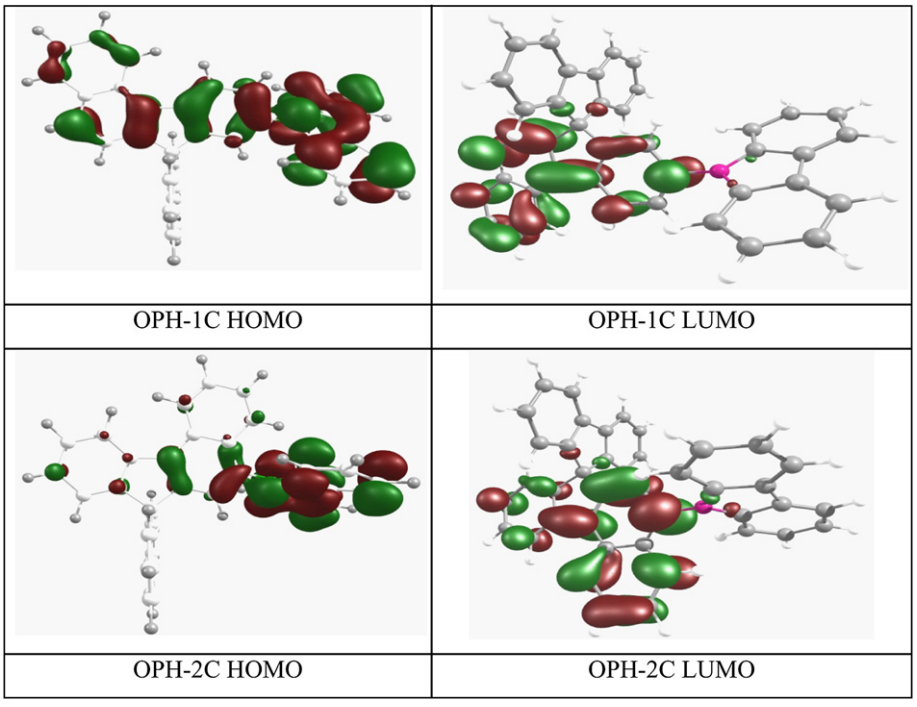

Fig. 5. Molecular orbital distribution of **OPH-1C** and **OPH-2C**.

Table 1
Thermal properties and EL properties of the devices obtained from two host and Ir(pq)$_2$acac dopant materials.

Properties	Devices	**OPH-1C**	**OPH-2C**
		Ir(pq)$_2$acac	
EL at 7 V	λ_{max} (nm)	596	596
	FWHM (nm)	70	73
	mA/cm^2	5.73	4.03
	cd/A[a]	17.1	15.4
	cd/A[b]	17.6 (6 V)	16.4 (6.5 V)
	lm/W[a]	8.47	7.62
	lm/W[b]	10.2 (6 V)	8.78 (6.5 V)
	cd/m^2	978.2	619.1
	CIE-x	0.595	0.587
	CIE-y	0.387	0.384
	EQE[a](%)	10.2	9.01
	EQE[b](%)	10.5 (6 V)	9.64 (6.5 V)
Thermal properties	T_g[c]	148 °C	142 °C
	T_m[d]	261 °C	371 °C
	T_d[e]	466 °C	458 °C

[a] Values at 7 V.
[b] Values at a peak.
[c] Glass transition temperature.
[d] Melting temperature.
[e] Decomposition temperature.

TGA data for the two host materials. The **OPH-1C** and **OPH-2C** hosts showed melting points (T_m) of 261 °C and 371 °C, respectively. On the second heating scan, no melting points were observed, even though they were given enough time to cool in air. Once they become amorphous solids, they do not revert to the crystalline state at all. After the samples had cooled to room temperature, a second DSC scan performed at 10 °C/min revealed high glass transition temperatures (T_g) of 148 °C and 142 °C for **OPH-1C** and **OPH-2C**, respectively, because of their rigid spiro-type backbone. This suggests that their thermal stability was significantly improved by the introduction of the carbazole group. As a result, the amorphous glassy state of the transparent films of the two host materials showed that they are good candidates for use as EL materials.

3.4. EL spectra

In order to find the optimum dopant concentration, the EL spectra of **OPH-1C** and **OPH-2C** doped by Ir(pq)$_2$acac dopant with different concentrations were gathered. The EL spectra of **OPH-1C** and **OPH-2C** red devices are shown in Fig. 6. All the devices showed typical EL spectra of Ir(pq)$_2$acac. The peak maximum of EL spectra was 596 nm and the spectra were red-shifted at high doping concentration. The EL emission is dominated by the emission peak of the Ir(pq)$_2$acac complex at around 595–601 nm. No host emission was observed in the devices. This seems to indicate that the energy transfer from the **OPH-1C** or **OPH-2C** host to the Ir(pq)$_2$acac complex is quite efficient at the optimum dopant concentration employed in this experiment. The full width at half maximum (FWHM 73 nm) is relatively small, which leads to good color purity as illustrated in PL spectrum. The dependence of the chromaticity on the current density was measured for the purpose of evaluating the stability of the devices as shown in Fig. 7. When the EL spectrum was converted into chromaticity coordinates on the CIE 1931 diagram, the stability of the chromaticity increased with an increase in the current density and the applied voltage. The stability of the CIEy coordinates was better than that of the CIEx. The **OPH-1C**-based device emits orange light having CIE coordinates of (0.595, 0.387). The stability of the color coordinates also increased with increasing dopant concentration.

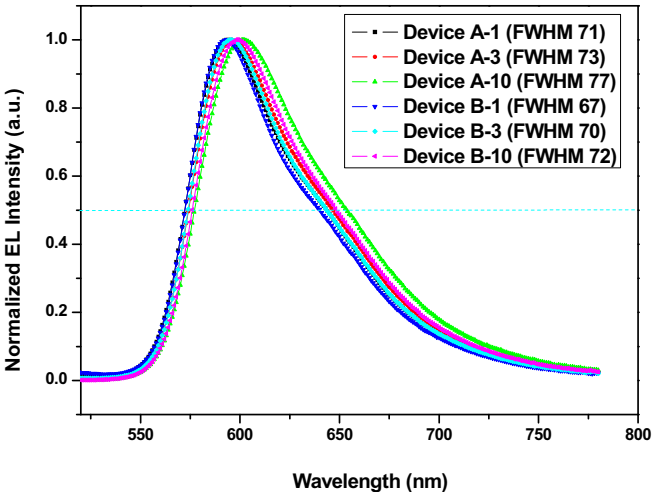

Fig. 6. EL spectra of the devices obtained from **OPH-1C** or **OPH-2C** host doped with various dopant materials.

3.5. OLED device properties

The multilayer diodes have a structure of ITO (150 nm)/DNTPD (60 nm)/NPB (30 nm)/**OPH-1C** or **OPH-2C**: Ir(pq)$_2$acac (30 nm, x %)/BCP (5 nm)/Alq$_3$ (20 nm)/LiF (1 nm)/Al (200 nm) (see Fig. 1). We fabricated six different multilayered devices. Devices A-1, A-3, and A-10 were fabricated with **OPH-1C** doped using 1%, 3% and 10% of Ir(pq)$_2$acac, respectively, while devices B-1, B-3 and B-10 made of the **OPH-2C** host were doped with 1%, 3% and 10% of Ir(pq)$_2$acac.

In Fig. 8, the maximum brightness of the LEDs was around 20,030 cd/m^2 (at 529 mA/cm^2) for the device A-1, 21,950 cd/m^2 (at 180 mA/cm^2) for device A-3 and 30,450 cd/m^2 (at 475 mA/cm^2) for device A-10. The current density and luminance of devices group A are lower than those of the devices group B. Especially, device A-10 showed the highest brightness of 30,450 cd/m^2, which is almost three times higher than that of device B-10. As the hole injection and transport through the **OPH-2C:** Ir(pq)$_2$acac layer is hindered with a decrease in the current density in the device due to the charge trapping by the dopant materials.

Fig. 9 displays the dependence of the luminance efficiency on the current density for the six phosphorescent devices with

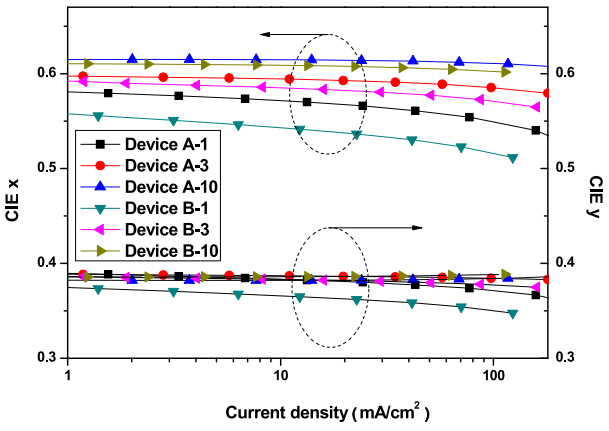

Fig. 7. Stability of the chromaticity depicted by CIE coordination.

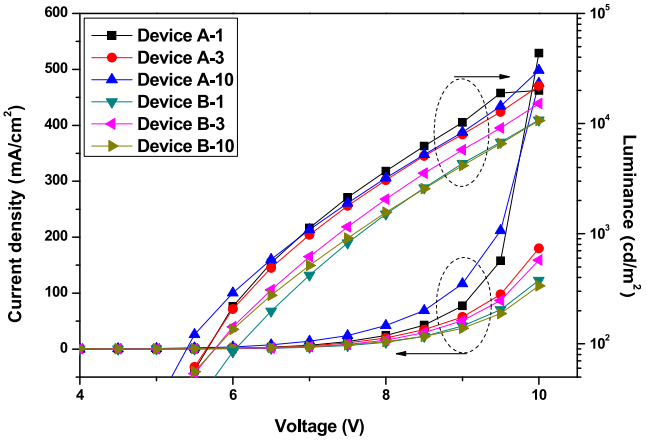

Fig. 8. Dependence of current density and luminance on the applied voltage.

different doping concentrations. The maximum luminance efficiencies of devices A-1, A -2, and A -3 were determined to be 16.6 cd/A (at 16.6 mA/cm^2), 17.6 cd/A (at 1.18 mA/cm^2) and 7.77 cd/A (at 3.73 mA/cm^2), respectively. Devices B-1, B-2, and B-3 made of the **OPH-2C** host exhibited lower luminance efficiency values than those made of **OPH-1C**. Device B-3 showed the highest luminance efficiency of around 16.4 cd/A (at 1.88 mA/cm^2) in the device B group. When the doping concentration was increased from 1 to 10 wt%, the luminance efficiency was decreased at a high doping concentration, due to the concentration quenching effect, and the maximum luminescence efficiency was obtained in the red OHOLED with a doping concentration of 3%. As a result, the device with **OPH-1C**: 3% Ir(pq)$_2$acac showed a luminance efficiency of 17.6 cd/A at 6 V and quantum efficiency of 10.5%. However a spirobenzofluorene based phosphine oxide compound with 10% doping concentration showed a quantum efficiency of 14.3% and a current efficiency of 20.4 cd/m^2 [34]. In the course of this work, similar orange host substituted carbazole at fluorene moiety has been reported to show a quantum efficiency of 8.3% [35]. In Fig. 10, the power efficiency increased abruptly at initial stage and followed by subsequent decrease in the performance of the 10wt%-doped device. Similar trends were observed for the devices with the different dopant concentration. The 3wt%-doped device exhibited

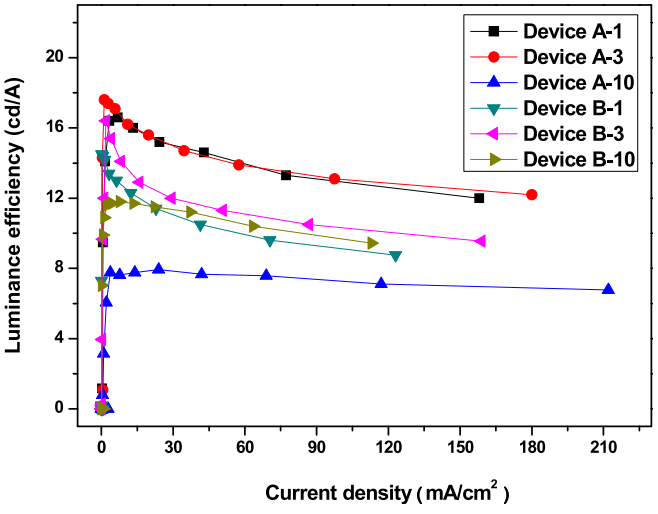

Fig. 9. Luminance efficiency–current density characteristics of the device using **OPH-1C** and **OPH-2C** Host.

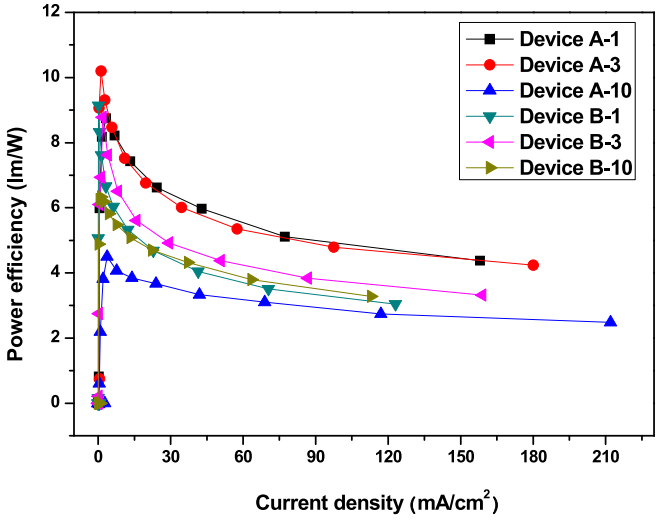

Fig. 10. Power efficiency–current density characteristics of the device using **OPH-1C** and **OPH-2C** Host.

the highest performance at 6 V with a maximum power efficiency of 10.2 lm/W at 1.18 mA/cm^2, which is ascribed to the larger number of excitons generated in the emitting layer. It is well known that the dipole–dipole interaction between randomly located and oriented dipoles is one of the major causes of energy disorder in organic materials [36]. At a very low dopant concentration in the EML layer, the average distance between the dopant molecules is mainly determined by the dipole–dipole interactions. Therefore, the dopant molecules in **OPH-1C** or **OPH-2C** with 10% dopant concentration create additional energy disorder, which leads to potential fluctuations caused by the dipole–dipole interactions of the randomly distributed dopant molecules.

4. Conclusion

A series of new orange light emitting spiro-type host materials, **OPH-1C** and **OPH-2C**, were successfully prepared by the amination reaction of 5 or 9-bromo-spiro[fluorene-7,9′-benzofluorene] with carbazole. When the device configuration of ITO/DNTPD/NPB/HOST: Ir(pq)$_2$acac/BCP/Alq$_3$/LiF/Al was constructed, the EL emissions of the devices (doped with 3% **OPH-1C**) were observed at 596 nm. The device obtained using **OPH-1C**:3% Ir(pq)$_2$acac showed a highest external quantum efficiency of 10.5% and CIE coordinates of (0.595, 0.387). According to these characteristics, these orange host emitting materials have the potential to be used for phosphorescent display applications.

Acknowledgements

This research was supported by WCU (World Class University) program through the National Research Foundation of Korea funded by the Ministry of Education, Science and Technology (R31-10069).

References

[1] Burroughes JH, Bradley DDC, Brown AR, Marks RN, Mackay K, Friend RH, et al. Light-emitting diodes based on conjugated polymers. Nature 1990;347:539–41.
[2] Tang CW, VanSlyke SA. Organic electroluminescent diodes. Applied Physics Letters 1987;51:913–5.
[3] Hung LS, Chen C. Recent progress of molecular organic electroluminescent materials and devices. Materials Science and Engineering: R: Reports 2002; 39:143–222.
[4] Mitschke U, Bäuerle P. The electroluminescence of organic materials. Journal of Materials Chemistry 2000;10:1471–508.

[5] Shirota Y. Organic materials for electronic and optoelectronic devices. Journal of Materials Chemistry 2000;10:1–26.
[6] Adachi C, Baldo M, Thompson ME, Forrest SR. Nearly 100% internal phosphorescence efficiency in an organic light-emitting device. Journal of Applied Physics 2001;90:5048–51.
[7] Hu B, Karasz F. Blue, green, red, and white electroluminescence from multichromophore polymer blends. Journal of Applied Physics 2003;93:1995–2001.
[8] Sun QJ, Hou JH, Yang CH, Li YF, Yang Y. Enhanced performance of white polymer light-emitting diodes using polymer blends as hole-transporting layers. Applied Physics Letters 2006;89:153501–3.
[9] Niu QL, Xu YH, Peng JB. Efficient polymer white-light-emitting diodes with a single-emission layer of fluorescent polymer blend. Journal of Luminescence 2007;126:531–5.
[10] Lee MT, Tseng MR. Efficient, long-life and Lambertian source of top-emitting white OLEDs using low-reflectivity molybdenum anode and co-doping technology. Current Applied Physics 2008;8:616–9.
[11] Aoki A, Tamagawa Y, Miyashita T. Effect of hole-transporting film thickness on the performance of electroluminescent devices using polymer Langmuir–-Blodgett films containing carbazole. Macromolecules 2002;35:3686–9.
[12] Kimoto A, Cho JS, Higuchi M, Yamamoto K. Synthesis of asymmetrically arranged dendrimers with a carbazole dendron and a phenylazomethine dendron. Macromolecules 2004;37:5531–7.
[13] Lu J, Tao Y, D'iorio M, Li Y, Ding J, Day M. Pure deep blue light-emitting diodes from alternating fluorene/carbazole copolymers by using suitable hole-blocking materials. Macromolecules 2004;37:2442–9.
[14] Hwang SW, Chen Y. Photoluminescent and electrochemical properties of Novel Poly(aryl ether)s with isolated hole-transporting carbazole and electron-transporting 1,3,4-oxadiazole fluorophores. Macromolecules 2002;35:5438–43.
[15] You Y, Kim SH, Jung HK, Park SY. Blue electrophosphorescence from iridium complex covalently bonded to the Poly(9-dodecyl-3-vinylcarbazole): suppressed phase segregation and enhanced energy transfer. Macromolecules 2006;39:349–56.
[16] Jiang J, Jiang C, Yang W, Zhen H, Huang F, Cao Y. High-efficiency electrophosphorescent fluorene-alt-carbazole copolymers N-grafted with cyclometalated Ir complexes. Macromolecules 2006;38:4072–80.
[17] Salbeck J, Yu N, Bauer J, Weissörtel F, Bestgen H. Low molecular organic glasses for blue electroluminescence. Synthetic Metals 1997;91:209–15.
[18] O'Brien DF, Burrows PE, Forrest SR, Konne BE, Loy DE, Thompson ME. Hole transporting materials with high glass transition temperatures for use in organic light-emitting devices. Advanced Materials 1998;10:1108–12.
[19] Katsuma AK, Shirota Y. Novel class of π-electron dendrimers for thermally and morphologically stable amorphous molecular materials. Advanced Materials 1998;10:223–6.
[20] Ko CW, Tao T. 9,9-Bis{4-[di-(p-biphenyl)aminophenyl]}fluorene: a high T_g and efficient hole-transporting material for electroluminescent devices. Synthetic Metals 2002;126:37–41.
[21] Salbeck J, Bauer J, Weissörtel F. Spiro linked compounds for use as active materials in organic light emitting diodes. Macromolecular Symposia 1997;125:121–32.
[22] Xiao H, Leng B, Tian H. Hole transport triphenylamine–spirosilabifluorene alternating copolymer: synthesis and optical, electrochemical and electroluminescent properties. Polymer 2005;46:5707–13.
[23] Xiao H, Shen H, Lin Y, Su J, Tian H. Spirosilabifluorene linked bistriphenylamine: synthesis and application in hole transporting and two-photon fluorescent imaging. Dyes and Pigments 2007;73:224–9.
[24] Katsis D, Geng YH, Ou JJ, Culligan SW, Trajkovska A, Chen SH, et al. Spiro-Linked Ter-, Penta-, and heptafluorenes as novel amorphous materials for blue light emission. Chemistry Materials 2002;14:1332–9.
[25] Bach U, Cloedt KD, Spreitzer H, Gratzel M. Characterization of hole transport in a new class of spiro-linked oligotriphenylamine compounds. Advanced Materials 2000;12:1060–3.
[26] Kim JH, Jeon YM, Jang JG, Ryu S, Chang HJ, Lee CW, et al. Blue OLEDs utilizing Spiro[fluorene-7,9′-benzofluorene]-type compounds as hosts and dopants. Bulletin Korean Chemical Society 2009;30:647–52.
[27] Jeon SO, Lee HS, Jeon YM, Kim JW, Lee CW, Gong MS. Electroluminescent properties of Spiro[fluorene-benzofluorene]-containing blue light emitting materials. Bulletin Korean Chemical Society 2009;30:863–8.
[28] Kim KS, Jeon YM, Kim JW, Lee CW, Gong MS. Blue light-emitting diodes from 2-(10-naphthylanthracene)-spiro[fluorene-7,9′-benzofluorene] host material. Dyes and Pigments 2009;81:174–9.
[29] Jeon YM, Kim JW, Lee CW, Gong MS. Blue organic light-emitting diodes using novel spiro[fluorene-benzofluorene]-type host materials. Dyes and Pigments 2009;83:66–71.
[30] Jeon SO, Jeon YM, Kim JW, Lee CW, Gong MS. Blue organic light-emitting diode with improved color purity using 5-naphthyl-spiro[fluorene-7,9′-benzofluorene]. Organic Electronics 2008;9:522–32.
[31] Kim KS, Jeon YM, Kim JW, Lee CW, Gong MS. Blue light-emitting OLED using new spiro[fluorene-7,9′-benzofluorene] host and dopant materials. Organic Electronics 2008;9:797–804.
[32] Jeon SO, Jeon YM, Kim JW, Lee CW, Gong MS. Spiro[fluorene-7,9′-benzofluorene] host and dopant materials for blue light-emitting electroluminescence device. Synthetic Metals 2009;159:1147–52.
[33] Cheon JW, Lee CW, Gong MS, Geum N. Chemiluminescent properties of blue 24 fluorophores containing naphthalene unit. Dyes and Pigments 2004;61:23–30.
[34] Jeon SO, Yook KS, Joo CW, Son HS, Jang SE, Lee JY. High efficiency red phosphorescent organic light-emitting diodes using a spirobenzofluorene type phosphine oxide as a host material. Organic Electronics 2009;10:998–1000.
[35] Jang SE, Jeon SO, Cho YJ, Yook KS, Lee JY. Stable efficiency roll-off in red phosphorescent organic light-emitting diodes using a spirofluorene–benzofluorene based carbazole type host material. Journal of Luminescence, 2010;130:2184–7.
[36] Dunlap DH, Parris PE, Kenkre VM. Charge-dipole model for the universal field dependence of mobilities in molecularly doped polymers. Physical Review Letters 1996;77:542–5.